

The Effect of Low-Intensity Pulsed Ultrasound on Bone-Tendon Junction Healing: Initiating After Inflammation Stage

Hongbin Lu,¹ Feifei Liu,¹ Huabin Chen,¹ Can Chen,¹ Jin Qu,¹ Daqi Xu,¹ Tao Zhang,¹ Jingyong Zhou,¹ Jianzhong Hu²

¹Department of Sports Medicine, Research Center of Sports Medicine, Xiangya Hospital, Central South University, Changsha 410008, China,

²Department of Spine Surgery, Research Center of Sports Medicine, Xiangya Hospital, Central South University, Changsha 410008, China

Received 10 August 2015; accepted 21 January 2016

Published online 18 February 2016 in Wiley Online Library (wileyonlinelibrary.com). DOI 10.1002/jor.23180

ABSTRACT: The purpose of this study was to explore the effect of low-intensity pulsed ultrasound (LIPUS) treatment initiating after inflammation stage on the process of bone-tendon junction (BTJ) healing in a rabbit model. Thirty-six rabbits undergoing partial patellectomy were randomly divided into two groups: control and LIPUS. The period of initial inflammatory stage is 2 weeks. So LIPUS treatment was initiated at postoperative week 2 and continued until the patella-patellar tendon (PPT) complexes were harvested at postoperative weeks 4, 8, and 16. At each time point, the PPT complexes were harvested for qRT-PCR, histology, radiographs, synchrotron radiation micro computed tomography (SR- μ CT), and biomechanical testing. The qRT-PCR results showed that LIPUS treatment beginning at postoperative week 2 played an anti-inflammatory role in BTJ healing. Histologically, the LIPUS group showed more advanced remodeling of the lamellar bone and marrow cavity than the control group. The area and length of the new bone in the LIPUS group were significantly greater than the control group at postoperative weeks 8 and 16. SR- μ CT demonstrated that new bone formation and remodeling in the LIPUS group were more advanced than the control group. Biomechanical test results demonstrated that the failure load, ultimate strength and energy at failure were significantly higher than those of the control group. In conclusion, LIPUS treatment beginning at postoperative week 2 was able to accelerate bone formation during the bone-tendon junction healing process and significantly improved the healing quality of BTJ injury. © 2016 The Authors. *Journal of Orthopaedic Research* published by Wiley Periodicals, Inc. on behalf of the Orthopaedic Research Society. *J Orthop Res* 34:1697–1706, 2018.

Keywords: low-intensity pulsed ultrasound (LIPUS); bone-tendon junction (BTJ); synchrotron radiation micro computed tomography (SR- μ CT)

The bone-tendon junction (BTJ) exists around the joints, where tendons or ligaments attach to bone and need a multi-tissue interface with spatial gradients to connect tissue, which can minimize stress concentrations and mediate load transfer between soft tissues and bone.¹ Injuries involving the BTJ around knee joint are common in sports exercise or vehicular trauma. The reattachment of bone to tendon is usually demonstrated to complete the repair of bone-tendon junction, for example, the repair between the patella and patellar tendon after transverse fractures or comminuted fractures.^{2,3} It has been reported that partial patellectomy had been performed in both clinical and experimental studies. Saltzman et al.² performed a standardized partial patellectomy on patients to treat patellar fracture, and confirmed the growth of the remaining patella by the follow-up of lateral radiographs. Qin et al.⁴ performed partial patellectomy in a rabbit model to study the BTJ repair, and discovered that the length of remaining patella could increase with healing over time.

Many surgeries in the field of sports medicine focus on the reconstruction of the BTJ. Compared with tendon-to-tendon or bone-to-bone healing, the repair of the BTJ is slower and more difficult because it is a transitional region composed of bone, fibrocartilage and tendon.^{5,6} It is impossible to completely recover morphological construct and physiological function after a severe injury of the BTJ.⁷ A long period of rest and immobilization is required before the functional recovery, and this can induce many complications, such as muscle atrophy, cartilage degeneration, and bone loss. Therefore, repair of the BTJ remains a significant clinical challenge. In addition to improving surgical techniques and post-operative rehabilitation, it is becoming increasingly important to discover a new therapy to promote BTJ healing in basic and clinical research.

As a noninvasive form of mechanical energy, low-intensity pulsed ultrasound (LIPUS) has been proven to be a safe and convenient adjuvant treatment to promote the recovery of musculoskeletal injuries.^{8–10} LIPUS can transcutaneously transmit high-frequency acoustical pressure waves and mechanical stress into biological tissues. It has been successfully proven to stimulate fracture healing and bone growth in both animal models and clinical trials.^{11–13} The ultrasound treatment was used in our previous studies and continued until the animals were euthanized. It has been reported that LIPUS is able to accelerate BTJ healing by promoting chondrogenesis, osteogenesis, and angiogenesis in a rabbit model.^{14–16} Our previous study¹⁶ showed that BTJ healing experienced the following four stages: an initial inflammatory stage, a newly formed bone with regenerated fibrocartilage zone-like structure stage, a woven bone remodeling and maturation of

This is an open access article under the terms of the Creative Commons Attribution-NonCommercial-NoDerivs License, which permits use and distribution in any medium, provided the original work is properly cited, the use is non-commercial and no modifications or adaptations are made.

Conflicts of interest: None.

The copyright line for this article was changed on July 27, 2018, after original online publication

Correspondence to: Jianzhong Hu (T: +86-731-84327174; F: +86-731-84327332; E-mail: jianzhonghu@hotmail.com)

© 2016 The Authors. *Journal of Orthopaedic Research* published by Wiley Periodicals, Inc. on behalf of the Orthopaedic Research Society.

fibrocartilaginous junction stage, and a final remodeling stage, which was similar to bone fracture healing. The period of initial inflammatory stage is 2 weeks.¹⁶ Although the effects of LIPUS treatment had been studied at day 3¹⁴ and 7¹⁷ after operation and proved the therapeutic effectiveness, but this study focused on the effect of LIPUS after the inflammation phase in order to optimize the initiating time of LIPUS treatment to promote the BTJ healing. It is well accepted that LIPUS can promote the fracture healing, but it may have some adverse effects, such as affecting the permeability of the cell membrane.^{18,19} In the acute stage of fracture, LIPUS may aggravate the inflammation around the normal cells by increasing the permeability.²⁰ In our previous studies, the initiating time of LIPUS treatment was located in the inflammation phase, so we hypothesized that delayed the initiation of LIPUS treatment could enhance healing of BTJ.

With the development of scanning and imaging technologies, SR- μ CT had been used in orthopedics, including in osteoarthritis,²¹ bone metastases,²² and osteoporosis.²³ There are many ways to measure the micro-architecture of bone, such as conventional μ CT, SR- μ CT. But compared with conventional μ CT, SR- μ CT has many advantages, such as possessing a monochromatic X-ray beam, a high photon flux and imaging resolutions, no beam-hardening effects, brilliant and small angular beam divergence and quantitative analysis of reconstruction.^{24,25} As a result, it will likely be popular with scientific researchers and clinicians in many fields. The innovation of this study lies in LIPUS treatment beginning at postoperative week 2 and using SR- μ CT to explore the effect of LIPUS on bone-tendon junction healing in a rabbit model.

We hypothesized that LIPUS treatment beginning at postoperative week 2 could accelerate new bone formation and remodeling at the BTJ. The objectives of the present study were to use an established partial patellectomy model in rabbits to explore the effect of LIPUS on the process of BTJ healing by qRT-PCR, histology, radiographs, SR- μ CT and biomechanical testing.

MATERIALS AND METHODS

We used 36 mature female New Zealand White rabbits (weight, 3.3 ± 0.2 kg) that underwent partial patellectomy on the right hind limb of each rabbit to establish the BTJ injury model according to experimental protocol previously described by Qin et al.⁴ Animals were divided into two groups: the LIPUS group (treated with LIPUS from postoperative week 2, $n = 18$) and the control group (treated with placebo, $n = 18$). During the experimental period, the animals were provided regular daily feeding and LIPUS treatment. Animals were sacrificed at postoperative weeks 4, 8, and 16 to harvest specimens. This study was approved by the Ethics Committee of the Center for Scientific Research with Animal Models of Central South University (No. 2012-06-04).

Animal Surgery and LIPUS Treatment

Animals were preoperatively anesthetized through intravenous injection with sodium pentobarbital (0.8 ml/kg, Merck,

Darmstadt, Germany). After preoperative skin preparation, disinfection and draping, an anterolateral skin incision was made on the right hind limb to expose the patella-patellar tendon (PPT) complex. All surgical procedures were performed under aseptic conditions. The positions of the proximal 2/3 and the distal 1/3 of the patella were first located, and a transverse osteotomy was then performed (Fig. 1A). The distal 1/3 of the patella was removed from the patellar tendon without the remaining fibrocartilage. Two holes were pre-drilled longitudinally in the proximal 2/3 of the patella before suturing the patellar tendon and the proximal patella with a 3–0 polydioxanone (PDS) suture (Mersilk, ETHICON Ltd, Edinburgh, UK) (Fig. 1B). A figure-of-eight tension band wire (diameter, 0.8 mm) was fixed between the top of the proximal patella and the tibial tuberosity to protect the PPT reconstruction (Fig. 1C). The surgical knee was immobilized with a long leg cast for 4 weeks after surgery, and then the immobilization was removed for free cage activity. In order to alleviate the pain and swelling, an analgesic (Tramadol, Grunenthal GmbH, Aachen, Germany) and an antibiotic (penicillin sodium, North China Pharmaceutical Co, Shijiazhuang, China) were administered for 3 days postoperatively. LIPUS was delivered to the surgical site from postoperative week 2 in the LIPUS group (20 min/day) until the animal was sacrificed. The control group received a placebo treatment. Animals were anaesthetized with 3% sodium pentobarbital before LIPUS treatment. The parameters of LIPUS (Exogen; Smith and Nephew, San Francisco, CA) delivery were adjusted to a 1.5 MHz frequency, 1:4 duty cycle and 30 mW/cm² spatial and temporal average incident intensity. No animals experienced accidental death in the experimental process.

Tissue Sample Preparation

Animals from both groups were sacrificed at week 4, 8, and 16 with an overdose of sodium pentobarbital according to the experimental plan. The number of rabbit was six for per group and per time point. The samples were immediately used for X-ray examination to evaluate the size of new bone when harvested at each time point. And then three samples were mid-sagittally cut into two halves, one half was stored in liquid nitrogen for qRT-PCR detection; the other half was fixed in neutral buffered formalin at 4°C for 24 h and then washed three times with a dual evaporate water for histological evaluation and SR- μ CT scanning. The other three intact samples were stored at -80°C for biomechanical testing.

qRT-PCR Assays

The mRNA expression levels of proinflammatory cytokines (TNF- α , IL-1 β , IL-6) and anti-inflammatory cytokines (TGF- β 1 and IL-10) were measured by qRT-PCR. The fresh PPT complexes collected at different time points were ground in liquid nitrogen. Total mRNA was extracted from the frozen PPT complexes using Trizol reagent (Invitrogen, Carlsbad, CA) at various time points. mRNA was resuspended in RNAase-free H₂O and stored at -80°C. mRNA was then subjected to synthesis of complementary DNA (cDNA) using the PrimeScriptTM RT reagent kit with gDNA Eraser (TaKaRa, Otsu, Japan). Samples were quantified simultaneously on a 96-well-plate using a real-time PCR detection system (Bio-Rad, Hercules, CA). qRT-PCR was performed using SYBR Premix Ex TaqTM (Tli RNaseH Plus) (TaKaRa, Otsu, Japan) with primers specific for TNF- α , IL-1 β , IL-6, IL-10, TGF- β 1, and GAPDH. The primer pairs were used for amplification as follows: TNF- α (forward, GCTACATCACCGAACCTCTG;

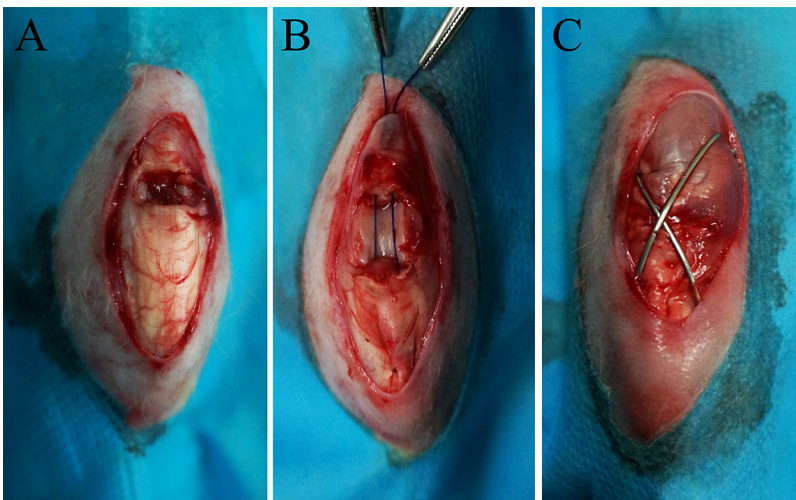


Figure 1. A diagram of the surgical procedure to establish the BTJ injury model in rabbits. (A) A transverse osteotomy was performed at the place of the proximal 2/3 and the distal 1/3 of the patella. (B) The distal 1/3 of the patella was removed (without remaining fibrocartilage), and then sutured the patellar tendon to the proximal patella. (C) A figure-of-eight tension band wire was fixed to protect the PPT reconstruction.

reverse, GAGTCTTTATTTCTCGCCACTGA), IL-1 β (forward, TCCAGACGAGGGCATCCA; reverse, CTGCCGGAAGCTCTTGTTG), IL-6 (forward, ATAATGAGACCTGCCTGCTGAG; reverse, TTCCTCGTCACTCCTGAACTTG), IL-10 (forward, CCTGTGTGGATTTGAGTGTCTTA; reverse, GCTCGGCTTAGGAGTTAGAAAG), TGF- β 1 (forward, CGGCAGCTGTACATTGACTT; reverse, AGCGCACGATCATGTTGGAC), and GAPDH (forward, ATGGTGAAGGTCGGAGTGAA; reverse, CGTGGGTGGAATCATACTGG). Amplification was performed via 1 cycle of 95°C for 30 s, 40 cycles of 95°C for 5 s, and 60°C for 30 s, followed by melt curve. The $2^{-\Delta\Delta Ct}$ method was used to analyze the gene expression value.

Histological Evaluation

The specimens were decalcified by 10% EDTA for 4 weeks to carry out histological analysis. After a series of graded ethanol dehydration (75%, 85%, 95%, and 100% twice for 4 h each), specimens were embedded in paraffin, then cut into 7- μ m-thick sections from the mid-sagittal plane using a rotary microtome (RM2165; Leica microsystems, Nussloch, Germany). Sections were stained with hematoxylin and eosin (HE) for the descriptive analysis of new bone and safranin O for the observation of cartilage-like tissue formation; the results were observed by light microscopy (Olympus CX31; Olympus Inc., Tokyo, Japan).

Radiographic Measurement

The PPT complexes were measured by a Faxitron MX-20 X-ray unit with high-resolution radiographs (Faxitron X-ray Corp, Lincolnshire, IL). The radiographs were captured with a 3 s exposure time and tube voltage at 40 kVp. The distance was set at 40 cm from the X-ray source to the object. The size of the newly formed bone was measured using the previous measurement protocol²⁶ after radiographs were analyzed by an image analysis system (Image-Pro Plus 6.0; Media Cybernetics Inc., MD).

SR- μ CT Imaging

The SR- μ CT scanning experiments were completed in the X-ray imaging and biomedical application beam line (BL13 W1) of the Shanghai Synchrotron Radiation Facility (SSRF) in China. The specimens were dehydrated through a series of graded ethanol (75%, 85%, 95% and 100% twice for 4 h each) before scanning. The beam energy was set as 18.0 keV with an exposure time of 0.5 s; the distance between the sample

and the detector was 5.0 cm. The CCD detector could catch the projection images with a pixel size of 3.25 μ m. The ring artifact was reduced by capturing dark-field and flat-field images. The obtained projection images were performed to phase retrieval, and they were converted into 8-bit slices by PITRE software reported by BL13W1.²⁶ Transverse slices were then transformed into 3D images by the VG Studio Max software (Ver.2.1 Volume Graphics GmbH, Germany). A fixed threshold was used to segment the gray-scale images in order to extract the bone phase before removing the noise by a median filter. BV/TV (bone volume fraction), Tb.N (trabecular number), Tb.Th (trabecular thickness), and Tb.Sp (trabecular separation) were used to compare the difference between two groups.

Mechanical Testing

The samples were thawed for 6 h before testing. The preparation included removing the soft tissue, band wire and suture around the PPT complexes. A Hounsfield test machine (H25k-S; Hounsfield Test Equipment Ltd) with a 2-kN load cell was used to detect the load to failure, ultimate strength, and energy to failure ratios. The width and thickness of the PPT complexes were measured with a caliper under the same tensile load (5N); the cross-sectional area (CSA) was calculated to compare the difference. The load to failure of the PPT complexes was tested at a rate of 20 mm/min with a preload of 1 N.

Statistical Analysis

All quantitative data were expressed as mean \pm standard deviation (SD), and two-way ANOVA was used to measure the effect of LIPUS treatment and healing time on BTJ healing, followed by post hoc Bonferroni multiple range tests for statistical differences. SPSS17.0 software was used to perform statistical analysis and $p < 0.05$ was considered to be statistically significant.

RESULTS

qRT-PCR Detection

Results from the qRT-PCR (Fig. 2) showed that the mRNA expression level of proinflammatory cytokines (TNF- α , IL-1 β , IL-6) decreased as the treatment time increased in both groups. Compared with the control group, the expression difference of TNF- α and IL-1 β

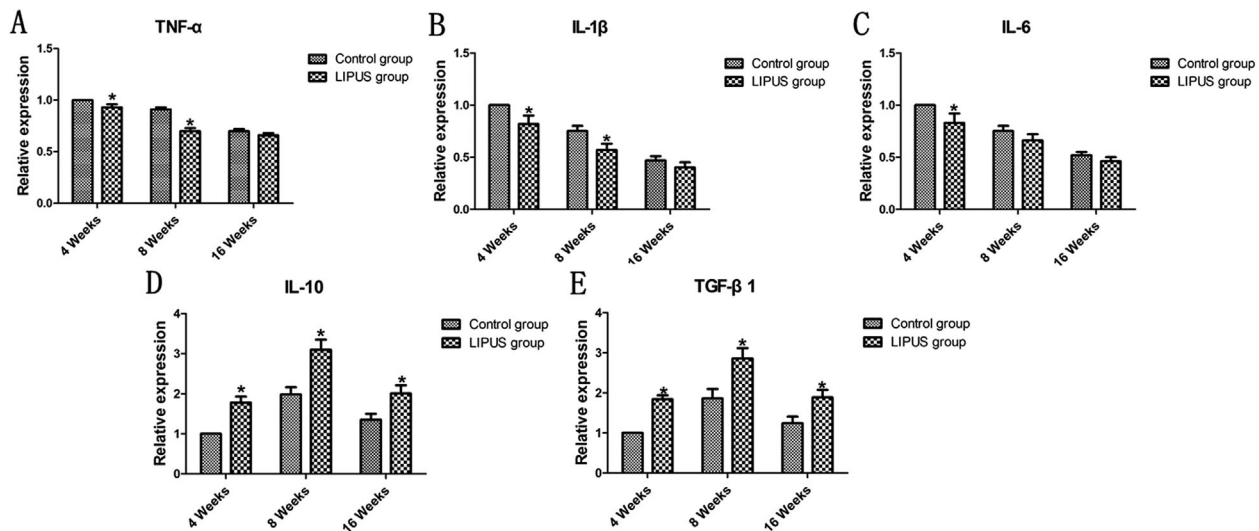


Figure 2. The mRNA expression of proinflammatory cytokines (A, B, C) and anti-inflammatory cytokines (D, E) in control and LIPUS groups. (* $p < 0.05$ the difference between the control and LIPUS groups).

was significantly different at postoperative weeks 4 and 8. The expressional difference of TNF- α was significant at week 8 ($p < 0.01$). The mRNA expression of IL-6 was significantly different only at week 4 ($p < 0.05$). In addition, no difference in the expression levels was observed between the groups at week 16. The mRNA expression of anti-inflammatory cytokines (TGF- β 1 and IL-10) increased in postoperative weeks 4 through 8, while it decreased in postoperative weeks 8 through 16; this suggests that the expression of anti-inflammatory cytokines reached its peak in both groups at postoperative week 8. The expression level of TGF- β 1 mRNA and IL-10 mRNA in the LIPUS group was greater than that of the control group at each time point. Therefore, it can be inferred that LIPUS promotes the expression of anti-inflammatory cytokines (TGF- β 1, IL-10) in the mid-healing stage and plays an anti-inflammatory role in the process of BTJ healing.

Descriptive Histology

During BTJ healing, endochondral ossification was the critical initiating stage after partial patellectomy. Results from H&E and safranin O staining (Figs. 3 and 4) indicated that neo-osteogenesis along with cartilage-like tissue were structurally connected to the remaining patella and tendon at the junction as the healing time increased in both groups. From the safranin O staining, cartilage-like tissue was found at the place of the newly formed bone and tendon, which was rich in proteoglycans. There was no apparent new bone and cartilage-like tissue found in either group at postoperative week 4, while the scar tissue as well as the fibrous tissue progressively formed between the remaining patella and tendon with healing over time. At postoperative week 8, new bone formation and cartilage-like tissue could be found in both groups with a clear boundary around the surface of the

osteotomy. The marrow cavity started to form, but it was less than that seen at postoperative week 16. At postoperative week 16, more new bone and cartilage-like tissue formation were found as outgrowth from the remaining patella in both groups. The cartilage-like tissue characterized with red distribution region, showed more proteoglycan than that of postoperative week 8. Compared with the control group, fibrocartilage cells were bigger and more mature in the LIPUS group. In addition, the LIPUS group specimens showed the change of the new trabecular bone pattern from woven bone to lamellar bone with well-aligned collagen fibers. Compared with the control group, the BTJ healing quality significantly improved in the LIPUS group because of more advanced remodeling of the lamellar bone and marrow cavity.

Radiographic Measurement

As the healing time increased, the newly formed bone and morphologic reshaping enlarged in both groups at each time point. The change of the area and length of the newly formed bone was obvious in the LIPUS group. Compared with the control group, there was more newly formed bone in the LIPUS group at postoperative week 8 (area: 3.00 ± 0.54 vs. 5.36 ± 0.84 , $p < 0.05$; length: 1.19 ± 0.20 vs. 1.85 ± 0.33 , $p < 0.05$) and 16 (area: 4.98 ± 0.98 vs. 8.24 ± 1.36 , $p < 0.05$; length: 2.12 ± 0.41 vs. 3.34 ± 0.49 , $p < 0.05$). However, no significant difference was found at postoperative week 4 (area: 1.82 ± 0.47 vs. 3.00 ± 0.59 , $p > 0.05$; length: 0.61 ± 0.15 vs. 0.95 ± 0.22 , $p > 0.05$) (Figs. 5 and 6).

3D Images by SR- μ CT

Our previous studies¹⁷ proved that SR- μ CT could be used to quantitatively evaluate the microarchitecture of new bone in the BTJ. Bone tissue was segmented after selecting the region of interest (ROI) of newly

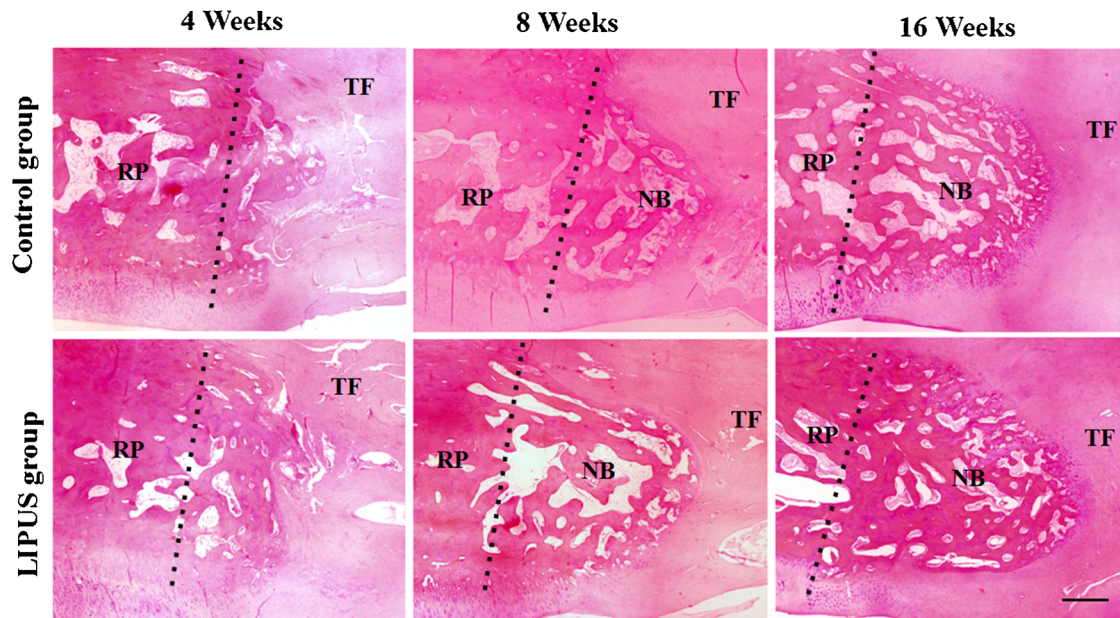


Figure 3. H&E-stained sagittal sections from the patella-patellar tendon at postoperative weeks 4, 8, and 16. New bone formation at the proximal patella was observed in both groups at postoperative weeks 8 and 16. The LIPUS group showed more trabecular and marrow cavities than the control group at postoperative week 16. The dotted line represents the surface of osteotomy (NB, newly formed bone; RP, remaining patella; TF, tendon fiber). Scanned bar = 1,000 μ m.

formed trabecular bone, and followed by acquiring the 3D images (Fig. 7). From the 3D reconstruction images, it was observed that new bone gradually formed and remodeled on the remaining patella as healing time increased. The ROI was placed in the center of the newly formed trabecular bone to reduce the effect of the region. The results in themorphological parameters showed that bone formation and reconstruction in the LIPUS group was superior to

the control group. At postoperative week 4, there was no significant difference in Tb.Th, Tb.N, Tb.Sp, and BV/TV between the control and LIPUS groups (Tb.Th: 47.51 ± 5.41 vs. $48.52 \pm 6.74 \mu$ m, $p > 0.05$; Tb.N: 2.75 ± 0.20 vs. 3.07 ± 0.35 1/mm, $p > 0.05$; Tb.Sp: 62.42 ± 7.76 vs. $57.64 \pm 6.76 \mu$ m, $p > 0.05$; BV/TV: 0.12 ± 0.03 vs. 0.14 ± 0.04 , $p > 0.05$). At postoperative week 8, Tb.Th, Tb.N and BV/TV of new bone in the LIPUS group were significantly higher than those of

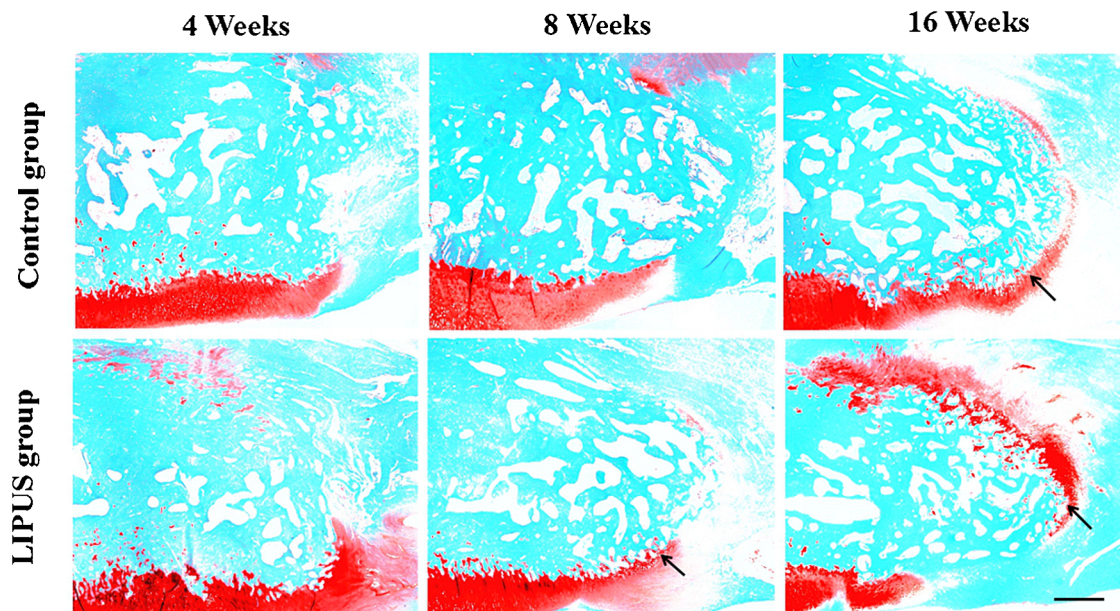


Figure 4. The safranin O staining showed the cartilage-like tissue formation (arrow) at bone-tendon junction. Proteoglycan was stained red by safranin O in the regenerated zone of cartilage-like tissue. With healing over time, more cartilage-like tissue was found at bone-tendon junction in both groups. Scanned bar = 1,000 μ m.

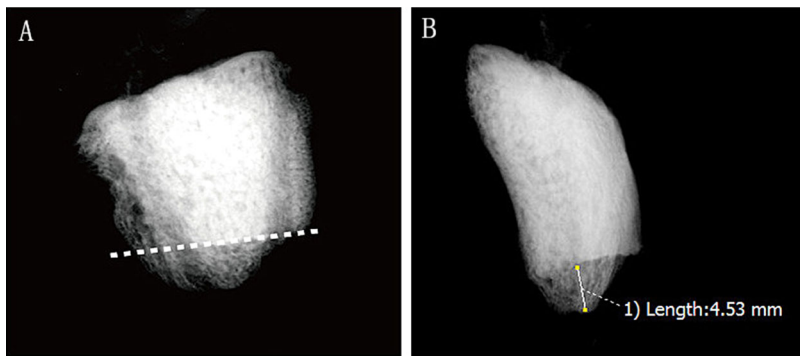


Figure 5. Measure of the size of the newly formed bone. (A) Anteroposterior digital radiographs of the patella. The dotted line represents the surface of osteotomy, and below it shows the area of the newly formed bone. (B) Lateral digital radiographs of the patella. The line between two points represents the length of the newly formed bone.

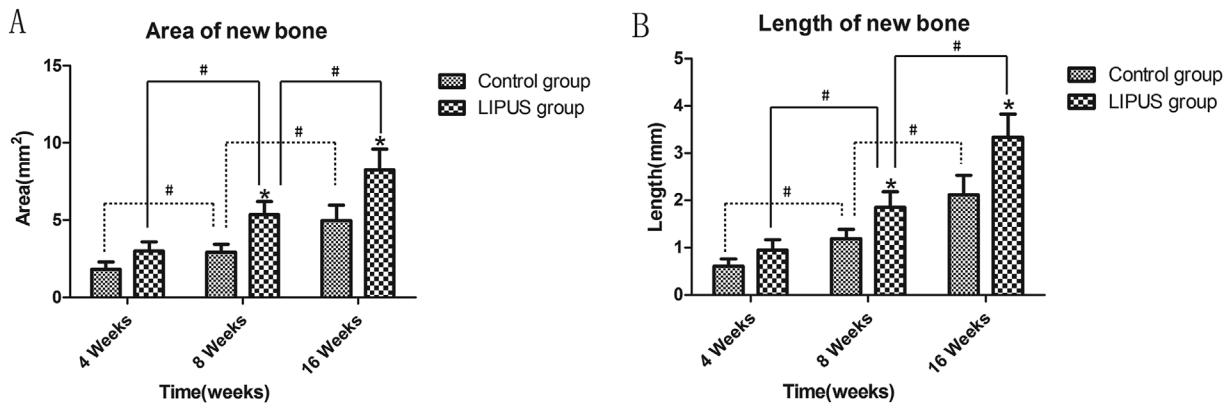


Figure 6. Comparison of the area (A) and length (B) of the newly formed bone between control and LIPUS groups at different time points. (* $p < 0.05$ the difference between control and LIPUS groups; # $p < 0.05$ the difference among different time points for control and LIPUS groups).

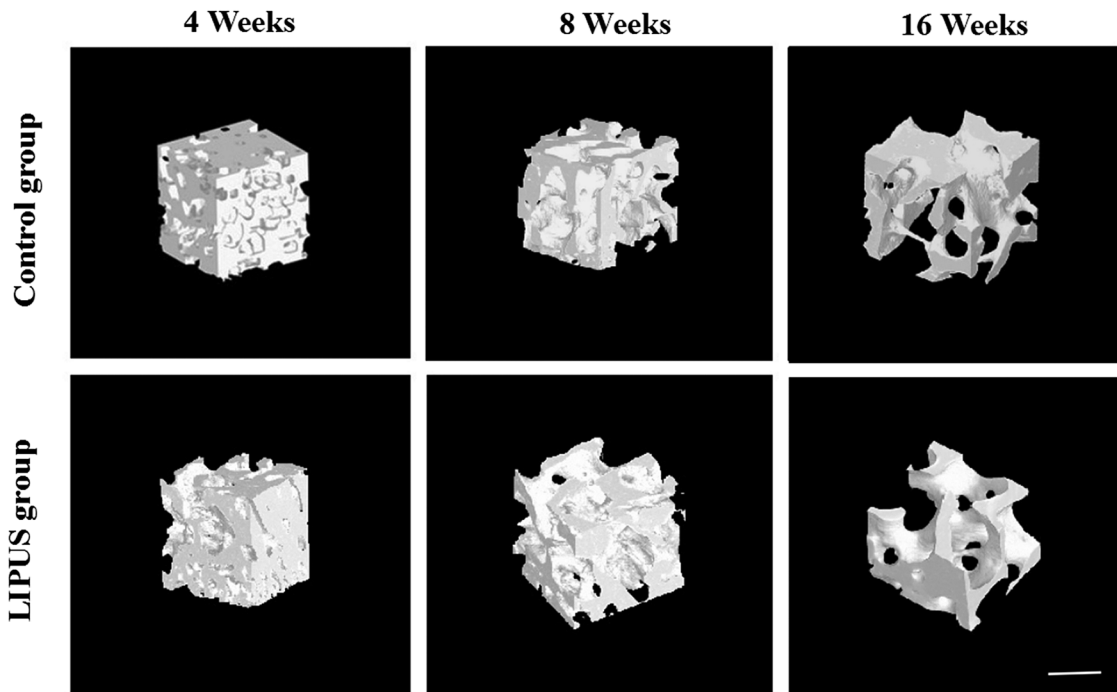


Figure 7. 3D tomographic reconstruction images of new trabecular bone located in the region of interest with high resolution. With the healing time increased, the new trabecular bone gradually became sparse because of marrow cavity formation. New bone formation and remodeling in the LIPUS group were more advanced than in the control group. Scanned bar = 1,000 μm .

the control group (Tb.Th: 77.11 ± 5.54 vs. 58.36 ± 4.15 , $p < 0.05$; Tb.N: 6.74 ± 0.50 vs. 4.69 ± 0.36 , $p < 0.05$; BV/TV: 0.60 ± 0.04 vs. 0.41 ± 0.03 , $p < 0.05$), while Tb.Sp in the LIPUS group was lower than in the control group (Tb.Sp: 97.10 ± 11.48 vs. 126.37 ± 11.21 , $p < 0.05$). At postoperative week 16, the difference was significant in Tb.Th and BV/TV between control and LIPUS groups (Tb.Th: 103.22 ± 5.34 vs. 119.57 ± 6.05 , $p < 0.05$; BV/TV: 0.47 ± 0.01 vs. 0.51 ± 0.02 , $p < 0.05$). No difference was found in the Tb.N and Tb.Sp of the new bone between two groups (Tb.N: 2.93 ± 0.16 vs. 3.15 ± 0.39 , $p > 0.05$; Tb.Sp: 166.52 ± 11.25 vs. 157.24 ± 12.55 , $p > 0.05$). Tb.Th and Tb.Sp of new bone increased from postoperative weeks 4–16. Tb.N and BV/TV increased from postoperative weeks 4 to 8 and Tb.N decreased from postoperative weeks 8–16. However, BV/TV increased in the control group and decreased in the LIPUS group from postoperative weeks 8–16 (Fig. 8).

Biomechanical Testing

The results of biomechanical testing (Table 1) demonstrated that the CSA, failure load, ultimate strength and energy at failure advanced with the healing over time and LIPUS improved these mechanical properties. Compared with the control group, there was a significantly smaller CSA of the PPT junction in the LIPUS group at postoperative weeks 8 and 16

($p < 0.05$). No difference in CSA was found in the LIPUS group between postoperative weeks 4 and 8 ($p > 0.05$), while the difference was significant in the control group ($p < 0.05$). In addition, no difference in CSA was found in the control group between postoperative weeks 8 and 16, while the difference was significant in the LIPUS group ($p < 0.05$). The results also showed significantly higher failure load, ultimate strength and energy at failure in the LIPUS group than in the control group at postoperative weeks 4, 8, and 16 ($p < 0.05$). The failure mode of the BTJ samples was observed at the place of osteotomy between the newly formed bone and the remaining patella after mechanical testing in both groups at postoperative week 8 and 16. While the failure mode of the BTJ samples was observed at the initial osteotomy site between the scar tissue and the remaining patella at postoperative week 4.

DISCUSSION

Our previous study demonstrated that LIPUS treatment accelerated the early angiogenesis by upregulated vascular endothelial growth factor (VEGF) and subsequent chondrogenesis in the process of BTJ healing, but the LIPUS treatment started at day 3 after surgery.¹⁶ Another previous research focused on the formation and remodeling of new trabecular bone, and quantitatively evaluate the microarchitecture of

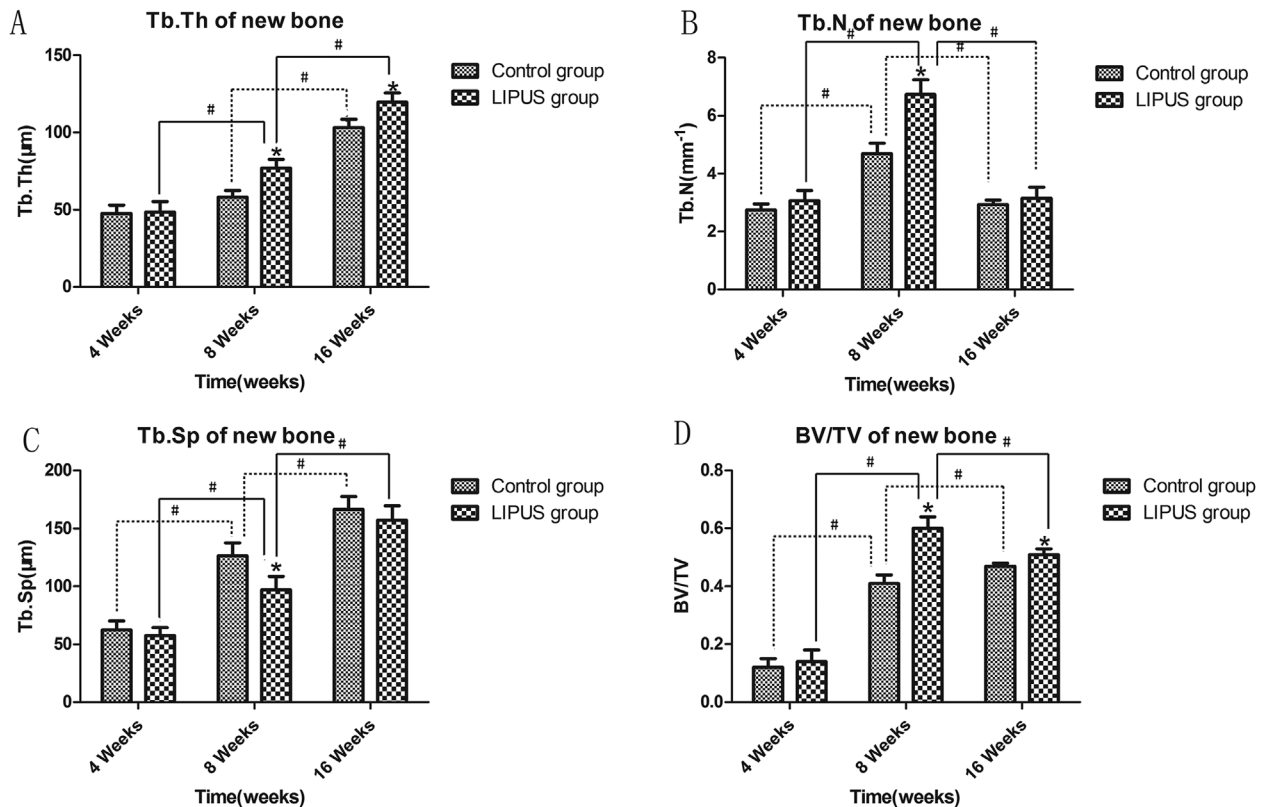


Figure 8. The morphological parameters of new bone in both groups. (A: Tb.Th, trabecular thickness; B: Tb.N, trabecular number; C: Tb.Sp, trabecular separation; D: BV/TV, bone volume fraction) ($p < 0.05$, the difference between control and LIPUS group at different time points; # $p < 0.05$, the difference between postoperative weeks 4 and 8 or weeks 8 and 16 within the same group).

Table 1. Crosssectional Area and Biomechanical Properties of the PPT Junction

	4 Weeks		8 Weeks		16 Weeks	
	Control	LIPUS	Control	LIPUS	Control	LIPUS
CSA (mm ²)	31.1 ± 2.9	24.3 ± 3.1	41.3 ± 3.0 ^b	29.6 ± 3.2 ^a	46.1 ± 3.2	37.9 ± 3.5 ^{a,c}
Failure load (N)	89.05 ± 15.48	131.86 ± 17.16 ^a	126.92 ± 26.66	203.19 ± 38.53 ^{a,b}	245.63 ± 32.68 ^c	408.00 ± 40.87 ^{a,c}
Ultimate strength (MPa)	3.11 ± 0.20	4.38 ± 0.37 ^a	3.88 ± 0.37 ^b	6.78 ± 0.44 ^{a,b}	6.77 ± 0.71 ^c	10.75 ± 0.74 ^{a,c}
Energy at failure (J)	0.16 ± 0.03	0.28 ± 0.04 ^a	0.25 ± 0.03 ^b	0.40 ± 0.04 ^{a,b}	0.56 ± 0.05 ^c	0.90 ± 0.08 ^{a,c}

LIPUS, low-intensity pulsed ultrasound; CSA, cross-sectional area; PPT, patella-patellar tendon.

All data are expressed as mean ± SD.

^aSignificant difference between LIPUS and control groups at the same time point ($p < 0.05$).

^bSignificant difference between postoperative weeks 4 and 8 in the same group ($p < 0.05$).

^cSignificant difference between postoperative weeks 8 and 16 in the same group ($p < 0.05$).

new trabecular bone. In addition, the LIPUS treatment was initiated at postoperative day 7.¹⁷ Although the effects of LIPUS treatment had been investigated at day 3 and 7 after operation, but this study focused on the delayed initiation of LIPUS treatment and explore the role of LIPUS in the BTJ healing by qRT-PCR detection, in order to optimize the initiating time of LIPUS treatment to promote the BTJ healing. The histological evaluation, radiographic measurement and SR- μ CT analysis as well as biomechanical testing showed that LIPUS treatment beginning at postoperative week 2 could accelerate BTJ healing as evidenced by more new bone formation and better mechanical properties.

Many cytokines, for example, IL-6, released in the early inflammatory stage of injury promoted mesenchymal stem cell release from the bone marrow into the blood and then accumulated at the injury site in favor of bone formation.²⁷ One of the proinflammatory cytokines, IL-1 β , played an important role in the production of inflammatory mediators, osteoclast formation, and matrix metalloproteinase activation.²⁸ We know that LIPUS can promote mRNA expression of TGF- β 1 and proteoglycan synthesis to promote bone repair.²⁹ qRT-PCR detection showed that proinflammatory cytokines (TNF- α , IL-1 β , IL-6) decreased as the healing time progressed, and their expression in the LIPUS group was lower than the control group. Moreover, there was no significant difference between the two groups at postoperative week 16. However, regardless of the group, anti-inflammatory cytokines (TGF- β 1 and IL-10) reached their peak at postoperative week 8. The expression of anti-inflammatory cytokines was higher in the LIPUS group than the control group at the three time points, while the expression of proinflammatory cytokines decreased from postoperative week 4–16 and was lower than the control group. A study was performed in a rat model of the surgical muscular incision to show that LIPUS decreased the blood counts of total leukocytes, and possessed the anti-inflammatory effect.³⁰ In a rat model of a ruptured Achilles tendon, LIPUS was also confirmed to increase expression of anti-inflammatory protein, such as TGF- β 1.³¹ We could

therefore deduce that LIPUS played a positive anti-inflammatory role in the process of BTJ healing.

The histological findings indicated that at the early stage of healing, only scar tissue and fibrous tissue were found; more new bone and cartilage-like tissue grew from the remaining patella in the LIPUS group than the control group with healing over time. Combined with the SR- μ CT data, more bone marrow cavities gradually formed from postoperative week 8–16. These were augmented with remodeling over time from dense woven bone to mature lamellar bone. The morphological parameters showed that the thickness of the trabecular bone increased with healing over time, while the separation increased with the formation of the marrow cavity. The number and bone volume fraction of the new trabecular bone decreased from postoperative weeks 8–16 in the LIPUS group because of remodeling. The remodeling of the new trabecular bone was more obvious from postoperative week 8 in the LIPUS group. We can therefore conclude that LIPUS accelerates new bone formation and advanced remodeling at the late stage of healing.

Based on previous *in vitro*³² and *in vivo*¹⁴ studies, LIPUS has been shown to be osteogenic. More new bone was formed in the distal edge of the remaining patella in the LIPUS group compared to the control group. Due to improving the remodeling of the scar tissue, the CSA was smaller in the LIPUS group than the control group. This was consistent with our previous studies.^{33,34} It was found that LIPUS promoted remodeling in the healing process of the PPT junction. Marder et al.³⁵ reported that new bone outgrowth from the remaining patella could decrease the contact pressure by increasing the patellofemoral contact area after partial patellectomy and improve the function of the knee joint. It was therefore not difficult to find that the area of new bone after partial patellectomy was obviously correlated with the postoperative functional recovery.^{2,36} Our previous study³⁷ found that the area and length of the new bone at the PPT junction after partial patellectomy correlated with functional properties, such as failure load, ultimate strength and energy at failure, and served as useful indices in assessing the quality of the BTJ healing. The load- and function-

induced remodeling process led to increases in area and length as well as the tensile properties of PPT. Therefore, the radiographic results suggest that LIPUS treatment beginning at postoperative week 2 could increase the area and length of the newly formed bone to improve the function of the knee.

Bone formation is a crucial stage in the process of BTJ healing.³⁸ The size of the new bone corresponded to the degree of healing in the process of BTJ healing.³⁹ From the radiographic results and histology, we can deduce that the size of new bone increased as the healing over time, more new bone and cartilage-like tissue were formed in the LIPUS group than the control group at the same time point. LIPUS was substantiated to possess the osteogenic effect by quantifications of the new bone area and length radiographically, which was consistent with our previous study.¹⁴ According to the failure mode of mechanical testing, failure was found at the newly formed bone and proximal patella rather than the new bone and the patellar tendon junction. This suggested that the weakest region was located at the initial osteotomy site. Therefore, the quality of bone remodeling at the proximal patella and the new bone was crucial to BTJ healing. Based on the Wolff's law, progressive weight-bearing and strength training was needed to improve the quality of remodeling.

The present study also had some inevitable limitations. Firstly, BTJ is a transitional region composed of bone, fibrocartilage and tendon. Many cell phenotypes across the interface of BTJ, so the result of gene expression may be affected by other cells in the tissue. Secondly, several markers of bone formation and bone remodeling should be carried out in the further study to illustrate the effect of new bone formation and remodeling by LIPUS. Thirdly, this study only explore the difference between the LIPUS group and control group, it will be performed a group with the LIPUS treatment starting immediately after operation to compare the difference of the LIPUS effect in the future study. Finally, a fine caliper was used to measure the width and thickness of the PPT complexes containing some soft tissue, but the measurement was easily affected by the pressure applied to the tissue, so the measurement must be repeated three times to reduce the error. In addition, the biomechanical testing was based on our previous study.^{14,40} The biomechanics presented is limited, as normalized properties were not measured.

CONCLUSIONS

LIPUS treatment beginning at postoperative week 2 accelerated the new bone formation and remodeling of new trabecular bone at the BTJ interface in a rabbit model, and significantly improved the healing quality of BTJ injury.

AUTHORS' CONTRIBUTIONS

HL and JH conceived and designed the study. HL, FL, HC, and CC completed the experiments. FL, DX,

JQ, and TZ analyzed the data. FL and JZ provided reagents/materials. HL and FL wrote the paper. The authors declare that they have read and approved submitting the manuscript.

ACKNOWLEDGMENTS

This study was supported by the National Natural Science Foundation of China (81171699 and 81472072) and Specialized Research Fund for the Doctoral Program of Higher Education of China (20110162110068).

REFERENCES

1. Lu HH, Thomopoulos S. 2013. Functional attachment of soft tissues to bone: development, healing, and tissue engineering. *Annu Rev Biomed Eng* 15:201–226.
2. Saltzman CL, Goulet JA, McClellan RT, et al. 1990. Results of treatment of displaced patellar fractures by partial patellectomy. *J Bone Joint Surg Am* 72:1279–1285.
3. Hung LK, Lee SY, Leung KS, et al. 1993. Partial patellectomy for patellar fracture: tension band wiring and early mobilization. *J Orthop Trauma* 7:252–260.
4. Qin L, Leung KS, Chan CW, et al. 1999. Enlargement of remaining patella after partial patellectomy in rabbits. *Med Sci Sports Exerc* 31:502–506.
5. Wang L, Qin L, Cheung WH, et al. 2010. A delayed bone-tendon junction healing model established for potential treatment of related sports injuries. *Br J Sports Med* 44:114–120.
6. Lui P, Zhang P, Chan K, et al. 2010. Biology and augmentation of tendon-bone insertion repair. *J Orthop Surg Res* 5:59.
7. Hope M, Saxby TS. 2007. Tendon healing. *Foot Ankle Clin* 12:553–567.
8. Waseem Z, Ford M, Syed K, et al. 2010. Chronic nonunion in a patient with bilateral supracondylar distal femur fractures treated successfully with twice daily low-intensity pulsed ultrasound. *PM R* 2:159–161.
9. Schofer MD, Block JE, Aigner J, et al. 2010. Improved healing response in delayed unions of the tibia with low-intensity pulsed ultrasound: results of a randomized sham-controlled trial. *BMC Musculoskelet Disord* 11:229.
10. Salem KH, Schmelz A. 2014. Low-intensity pulsed ultrasound shortens the treatment time in tibial distraction osteogenesis. *Int Orthop* 38:1477–1482.
11. Pounder NM, Harrison AJ. 2008. Low intensity pulsed ultrasound for fracture healing: a review of the clinical evidence and the associated biological mechanism of action. *Ultrasonics* 48:330–338.
12. Hannemann PF, Mommers EH, Schots JP, et al. 2014. The effect of low-intensity pulsed ultrasound and pulsed electromagnetic fields bone growth stimulation in acute fractures: a systematic review and meta-analysis of randomized controlled trials. *Arch Orthop Trauma Surg* 134:1093–1106.
13. Fung CH, Cheung WH, Pounder NM, et al. 2012. Effects of different therapeutic ultrasound intensities on fracture healing in rats. *Ultrasound Med Biol* 38:745–752.
14. Lu H, Qin L, Fok P, et al. 2006. Low-intensity pulsed ultrasound accelerates bone-tendon junction healing: a partial patellectomy model in rabbits. *Am J Sports Med* 34:1287–1296.
15. Qin L, Lu H, Fok P, et al. 2006. Low-intensity pulsed ultrasound accelerates osteogenesis at bone-tendon healing junction. *Ultrasound Med Biol* 32:1905–1911.
16. Lu H, Qin L, Cheung W, et al. 2008. Low-intensity pulsed ultrasound accelerated bone-tendon junction healing through regulation of vascular endothelial growth factor expression and cartilage formation. *Ultrasound Med Biol* 34:1248–1260.

17. Lu H, Zheng C, Wang Z, et al. 2015. Effect of low-intensity pulsed ultrasound on new trabecular bone during bone-tendon junction healing in a rabbit model: a synchrotron radiation micro-CT study. *PLoS ONE* 10:e1124724.
18. Guzman HR, Nguyen DX, Khan S, et al. 2001. Ultrasound-mediated disruption of cell membranes. I. Quantification of molecular uptake and cell viability. *J Acoust Soc Am* 110:588–596.
19. Guzman HR, Nguyen DX, Khan S, et al. 2001. Ultrasound-mediated disruption of cell membranes. II. Heterogeneous effects on cells. *J Acoust Soc Am* 110:597–606.
20. Zhao X, Yan SG. 2011. Low-intensity pulsed ultrasound (LIPUS) therapy may enhance the negative effects of oxygen radicals in the acute phase of fracture. *Med Hypotheses* 76:283–285.
21. Chappard C, Peyrin F, Bonnassie A, et al. 2006. Subchondral bone micro-architectural alterations in osteoarthritis: a synchrotron micro-computed tomography study. *Osteoarthritis Cartilage* 14:215–223.
22. Sone T, Tamada T, Jo Y, et al. 2004. Analysis of three-dimensional microarchitecture and degree of mineralization in bone metastases from prostate cancer using synchrotron microcomputed tomography. *Bone* 35:432–438.
23. Okazaki N, Chiba K, Taguchi K, et al. 2014. Trabecular microfractures in the femoral head with osteoporosis: analysis of microcallus formations by synchrotron radiation micro CT. *Bone* 64:82–87.
24. Jorgenson BL, Buie HR, McErlain DD, et al. 2015. A comparison of methods for in vivo assessment of cortical porosity in the human appendicular skeleton. *Bone* 73:167–175.
25. Chappard C, Basillais A, Benhamou L, et al. 2006. Comparison of synchrotron radiation and conventional x-ray microcomputed tomography for assessing trabecular bone microchitecture of human femoral heads. *Med Phys* 33:3568–3577.
26. Chen RC, Dreossi D, Mancini L, et al. 2012. PITRE: software for phase-sensitive X-ray image processing and tomography reconstruction. *J Synchrotron Radiat* 19:836–845.
27. Bastian O, Pillay J, Alblas J, et al. 2011. Systemic inflammation and fracture healing. *J Leukoc Biol* 89:669–673.
28. Graves DT, Cochran D. 2003. The contribution of interleukin-1 and tumor necrosis factor to periodontal tissue destruction. *J Periodontol* 74:391–401.
29. Mukai S, Ito H, Nakagawa Y, et al. 2005. Transforming growth factor-beta1 mediates the effects of low intensity pulsed ultrasound in chondrocytes. *Ultrasound Med Biol* 31:1713–1721.
30. Signori LU, Costa ST, Neto AF, et al. 2011. Haematological effect of pulsed ultrasound in acute muscular inflammation in rats. *Physiotherapy* 97:163–169.
31. Kosaka T, Masaoka T, Yamamoto K. Possible molecular mechanism of promotion of repair of acute Achilles tendon rupture by low intensity-pulsed ultrasound treatment in a rat model. *Weat Indian Med J* 60:263–268.
32. Tam KF, Cheung WH, Lee KM, et al. 2008. Osteogenic effects of low-intensity pulsed ultrasound, extracorporeal shockwaves and their combination-an in vitro comparative study on human periosteal cells. *Ultrasound Med Biol* 34:1957–1965.
33. Leung KS, Qin L, Fu LK, et al. 2002. A comparative study of bone to bone repair and bone to tendon healing in patella-patellar tendon complex in rabbits. *Clin Biomech* 17:594–602.
34. Hu J, Qu J, Xu D, et al. 2014. Combined application of low-intensity pulsed ultrasound and functional electrical stimulation accelerates bone-tendon junction healing in a rabbit model. *J Orthop Res* 32:204–209.
35. Marder RA, Swanson TV, Sharkey NA, et al. 1993. Effects of partial patellectomy and reattachment of the patellar tendon on patellofemoral contact areas and pressures. *J Bone Joint Surg Am* 75:35–45.
36. Fazzalari NL. 2011. Bone fracture and bone fracture repair. *Osteoporos Int* 22:2003–2006.
37. Lu H, Hu J, Qin L, et al. 2011. Area, length and mineralization content of new bone at bone-tendon junction predict its repair quality. *J Orthop Res* 29:672–677.
38. Huangfu X, Zhao J. 2007. Tendon-bone healing enhancement using injectable tricalcium phosphate in a dog anterior cruciate ligament reconstruction model. *Arthroscopy* 23:455–462.
39. Cakici H, Hapa O, Ozturan K, et al. 2010. Patellar tendon ossification after partial patellectomy: a case report. *J Med Case Rep* 4:47.
40. Xu D, Zhang T, Qu J, et al. 2014. Enhanced patella-patellar tendon healing using combined magnetic fields in a rabbit model. *Am J Sports Med* 42:2495–2501.